Studies in Photoelastic Stress Distributions, Modulusli of Flexural Elasticity and Displacement on Simple Beam Models Constructed of Epoxy Resin with Some Different Heights and Supported Conditions

Studies in Photoelastic Stress Distributions, Modulusli of Flexural Elasticity and Displacement on Simple Beam Models Constructed of Epoxy Resin with Some Different Heights and Supported Conditions

Sakutaro Nakamura*

Abstract

By using epoxy resin the present writer has made 15 beam models shown in Fig. 1 that are constructed with three kinds of different supported constructions and five kinds of different heights.

Then, he has supported simply each the above-mentioned beam models and increased gradually a concentrated line load on the centre of span and by means of Photo-Elasticity Apparatus, Reading Microscope and Strain Meter he has measured and analyzed experimentally the stress distributions of some cross sections τ_{yx}, σ_x, σ_y and the verticl and horizontal displacements and the maximum tensile and compressive stress intensties, and has made a comparative study of those.

I. Introduction

Some studies are already published by Mr. Coker, Filon, Fukuhara, Frocht, Wilson, Stokes, Boussinesq, Lamb and the other research workers on the general stress phenomenon of the simple deep beam.

Already the present writer has clarified the delicate change of stress distribution phenomena at the various extent of ratio of the height of cross section (h) to the span (1)—h/l, and by receiving a hint from those investigated results he has recently had a strong desire to investigate the influence of some different heights and constructions of supported points.

Then, he has studied also the changeable phenomena of stress distributions and displacements of simple beam models at the various extent of the equantity of load.

The stress phenomenon of extremely deep beams of immense height for the span caused public discussions too at the field of architectural constructions, and Mr. Karl Girkmann and Kurt Beyer discussed in their aleady published books that the solution of deep beam in the case of $h/l>0.50$ was not satisfied by the Common Beam Theory and was satisfied only by the Theory of Scheibe.

The above-mentioned consideration has been proved by the investigative results of the present writer and he has defined the boundary values, $h/l \fallingdotseq 0.50$ within the limits of possibility applying the Common Beam Theory.

Then in the case of $h/l=0.50$, we must consider carefully whether to select either of the Beam Theory or the Scheibe Theory, because the stress distributions and displacements change delicately on the ground of the supporting and loading conditions.

---

* 中村作太郎

In each case of the solution with the Beam Theory or the Scheibe Theory as the main constituents, we must add respectixely the secondary stress influence of plate or the primary stress influence of beam.

The defect of Beam Theory or Scheibe Theory is due to the want of the secondary strict stress distributions or the primary exact horizontal and vertical displacements.

It seems still more so that the analytical solution of simple deep beam by applying the Scheibe Theory in the consideration of general supporting and loading conditions is very ideal and hard and the calculating realization of those is very difficult.

Recently Mr. E. Mönch, J. P. Lee and П. И. Ааексеев have published in foreign periodicals concerning the deep beam, but those reports are only partial News Record and do not refer to fundamental problem that the present writer regards as important.

Moreover, there are no dissertations on those fundamental problems of deep beam within his knowlege.

The experimental analyses made by Mr. Coker, Filon, Frocht and Fukuhara were teated on the stress distribution as the main constituents and not treated on the accurate measurements of displacements.

The results of their experiments do not enable us to discuss the exact stress phenomena and displacements.

From the above-metioned viewpoint, the present writer has made by using epoxy resin 15 beam models shown in Fig. 1 that are constructed with three kinds of

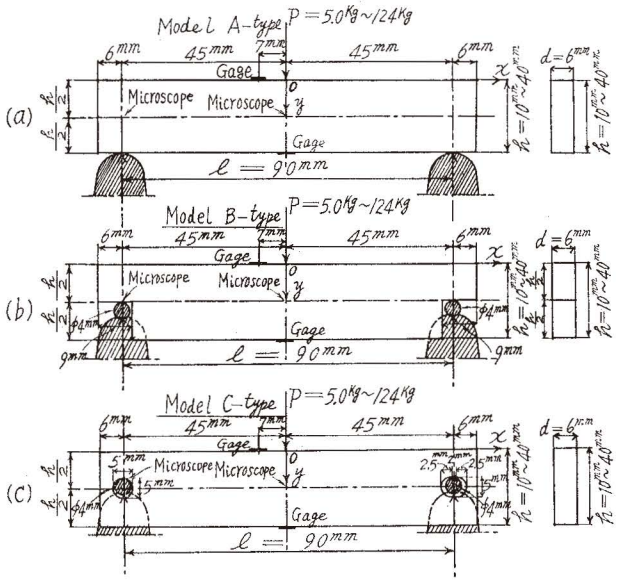

Fig. 1. Dimension Details Connected with the Supported Constructions, the Loading Point and Cross Sections of Some Simple Beam Models Constructed of Epoxy Resin.

different supported constructions and five kinds of different heights.

Then, he has supported simply each the avobe-mentioned beam models and increased gradually a concentrated line load on the centre of span and by means of Photo-Elasticity Apparatus (Riken Standard Type), Reading Microscope (Shimazu A Type) and Strain Meter he has measured and got the stress distributions of some cross sections τ_{yx}, σ_x, σ_y and the virtical and horizontal displacements and the maximum tensile and compressive stress intensities.

Still more from these results, he has got the curves of $\sigma_{max}/\sigma_{nom}-l/h$, Load-Deflection Curves and Stress-Strain Curves at the centre of span, and the curves of E_b-l/h and he clarified the relation of the stress and displacement phenomena.

He calculated the values of expansion and contraction at the central axis by using the horizontal displacements of supported point on the central axis and considered also the deformations of beam models.

Then, he has compared the results of experimental analysis with the theoretical calculating values and clarified the difference between those, and observed also the breaking phenomenon of models by increasing a concentrated line load.

II. The Experiment of Models and Its Analytical Theory

1. On models

The present writer has used the epoxy resin plates of thickness 6 mm by the good office of Riken Meter Company as the materials of beam models.

In making the models, he has taken especial care of the prevention of measuring

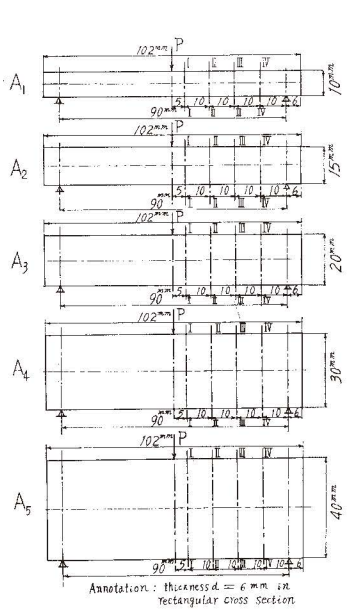

Fig. 2. Dimension Details of the A-Type Beam Models.

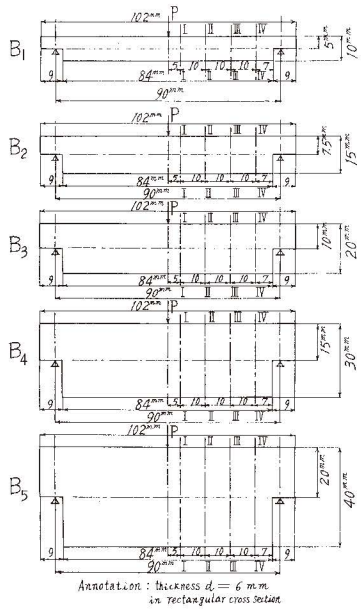

Fig. 3. Dimension Details of the B-Type Beam Models.

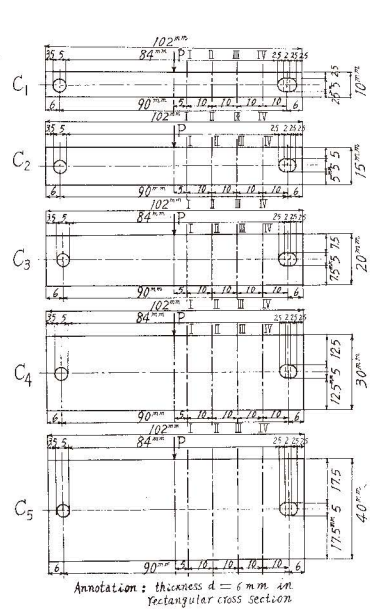

Fig. 4. Dimension Details of the C-Type Beam Models.

errors and processing distortions and given the manual finishing touches by using some files to put down maximnm allowable errors less than 2%.

Then, he has experimented quickly as soon as the models are finished before the initial stresses of time effect occur in the models.

The shapes and dimensions of models are shown in Fig. 2, 3, 4.

Moreover, he has made an experiment on the photoelastic property of models A_1, A_2, A_3 and got the values of the fringe stress $S=1.0738$ kg/mm and the photoelastic sensitivity $\alpha=0.9636$ mm/kg on the section I—I of each models by using the formulae $S=\sigma d/n=12\,M/(h^2N)$, $\alpha=l/S$ (d: thickness of model, n: degree of stress patterns, N: total of n).

2. Method of experiments

On the loading support of Photo-Elasticity Apparatus he has laid in the state of simple supported beam one by one 15 beam models that consist of the A-type beam models A_1, A_2, A_3, A_4, A_5, the B-type beam models B_1, B_2, B_3, B_4, B_5 and the C-type beam models C_1, C_2, C_3, C_4, C_5.

Next, he has put a concentrated line load on the upper surface of the centre of span as showing in Fig. 1 and taken the photoelastic photographs of stripe-patterns by using a source of mercurial light.

Then, he has decreased suitably a concentrated line load and plotted the inclined lines at intervals of 10 degrees on a tracing paper stretched upon a screen by using a source of white light.

He has pasted the gages of KP-18, Resistance $120.1\pm0.3\%$ and Gage Facter $1.94\pm1.0\%$ on the upper and lower surface of each model at the centre of span as Fig. 1 and measured its fibre strains by using a strain meter.

He has used two Reading Microscopes and measured at the same time the horizontal and vertical displacements on the central axis of each model at the central and supported points of span.

3. Experimental analyses

The stress pattern and isoclinics are shown in Fig. 5～Fig. 19.

Model A_1 ($h=1.0$ cm, $l=9.0$ cm)

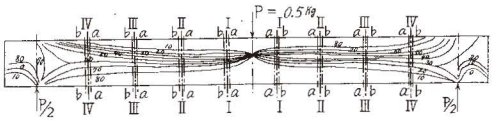

(a) Isoclinics in the Case of $P=0.5$ kg

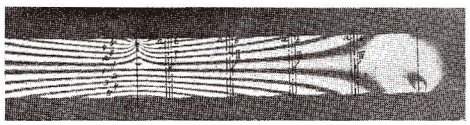

(b) Stress Patterns in the Case of $P=5.0$ kg

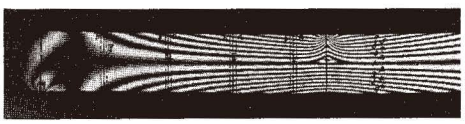

(c) Stress Patterns in the Case of $P=7.5$ kg

Fig. 5. Isoclinics and Stress Patterns of the Beam Model A_1 Bearing a Concentrated Line Lood.

Model A_2 ($h=1.5$ cm, $l=9.0$ cm)

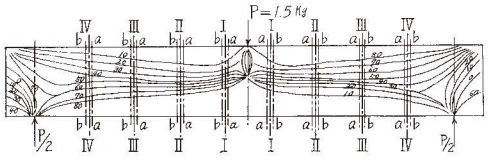

(a) Isoclinics in the Case of P=1.5 kg

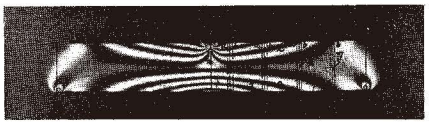

(b) Stress Patterns in the Case of $P=10.0$ kg

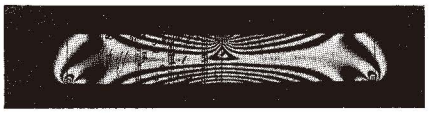

(c) Stress Patterns in the Case of $P=12.5$ kg

Fig. 6. Isoclinics and Stress Patterns of the Beam Model A_2 Bearing a Concentrated Line Load.

Model A_3 ($h=2.0$ cm, $l=9.0$ cm)

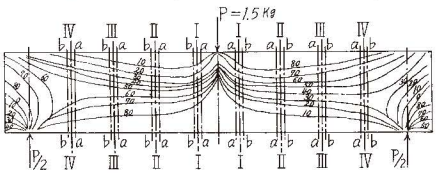

(a) Isoclinics in the Case of $P=1.5$ kg

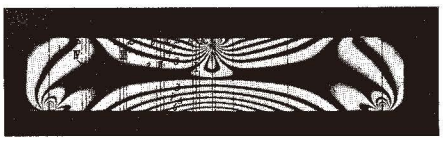

(b) Stress Patterns in the Case of $P=25.0$ kg

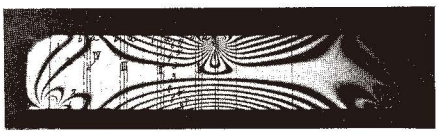

(c) Stress Patterns in the Case of $P=32.5$ kg

Fig. 7. Isocliinics and Stress Patterns of the Beam Model A_3 Bearing a concentrated Line Load.

Model A_4 ($h=2.0$ cm, $l=9.0$ cm)

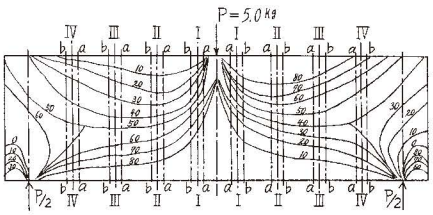

(a) Isoclinics in the Case of $P=5.0$ kg

(b) Stress Patterns in the Case of $P=40.0$ kg

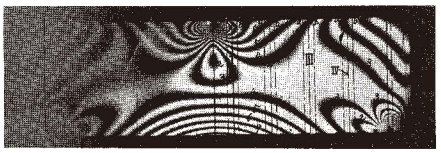

(c) Stress Patterns in the Case of $P=70.0$ kg

Fig. 8. Isoclinics and Stress Patterns of the Beam Model A_4 Bearing a Concentrated Line Load.

Model A_5 ($h=4.0$ cm, $l=9.0$ cm)

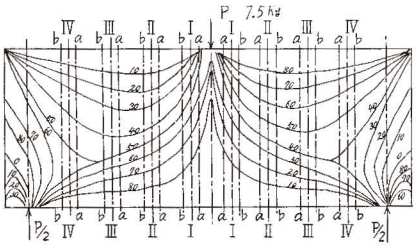

(a) Isoclinics in the Case of $P=7.5$ kg

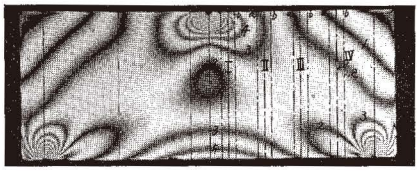

(b) Stress Patterns in the Case of $P=70.0$ kg

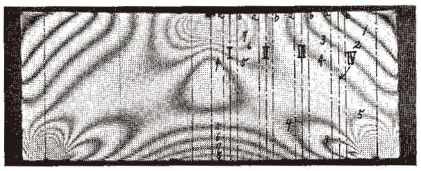

(c) Stress Patterns in the Case of $P=124.0$ kg

Fig. 9. Isoclinics and Stress Patterns of the Beam Model A_5 Bearing a Concentrated Line Load·

Model B_1 ($h=1.0$ cm, $l=9.0$ cm)

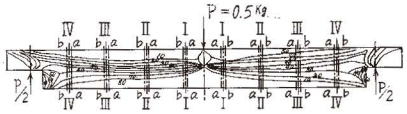

(a) Isoclinics in the Case of $P=0.5$ kg

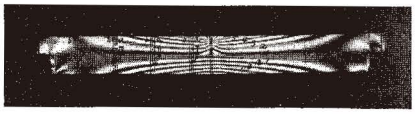

(b) Stress Patterns in the Case of $P=5.0$ kg

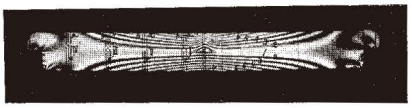

(c) Stress Patterns in the Case of $P=7.5$ kg

Fig. 10. Isoclinics and Stress Patterns of the Beam Model B_1 Bearing a Concentrated Line Load

Model B_2 ($h=1.5$ cm, $l=9.0$ cm)

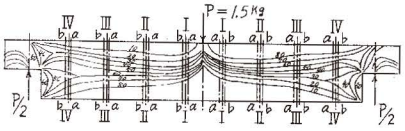

(a) Isoclinics in the Case of $P=1.5$ kg

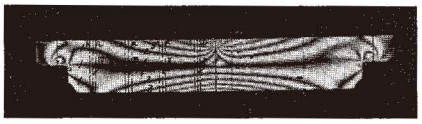

(b) Stress Patterns in the Case of $P=10.0$ kg

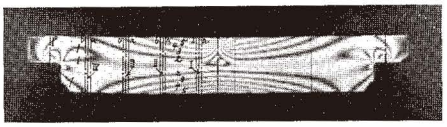

(c) Stress Patterns in the Case of $P=12.5$ kg

Fig. 11. Isoclinics and Stress Patterns of the Beam Model B_2 Bearing a Concentrated Line Load.

Model B_3 ($h=2.0$ cm, $l=9.0$ cm)

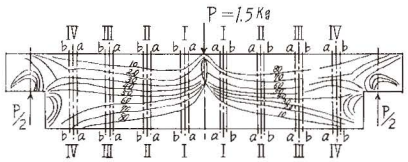

(a) Isoclinics in the Case of $P=1.5$ kg

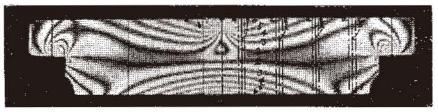

(b) Stress Patterns in the Case of $P=25.0$ kg

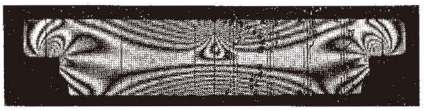

(c) Stress Patterns in the Case of $P=32.5$ kg

Fig. 12. Isoclinics and Stress Patterns of the Beam Model B_3 Bearing a Concentrated Line Load.

Model B_4 ($h=3.0$ cm, $l=9.0$ cm)

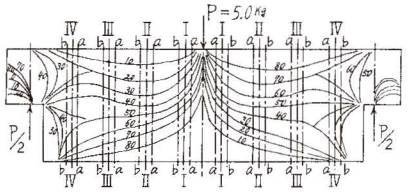

(a) Isoclinics in the Case of $P=5.0$ kg

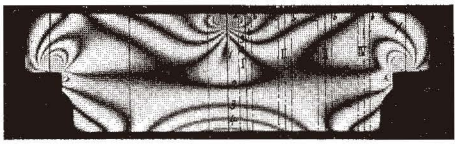

(b) Stress Patterns in the Case of $P=40.0$ kg

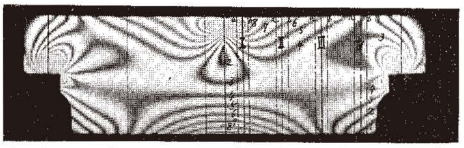

(c) Stress Patterns in the Case of $P=70.0$ kg

Fig. 13. Isoclinics and Stress Patterns of the Beam Model B_4 Bearing a Concentrated Line Load.

Model B_5 ($h=4.0$ cm, $l=9.0$ cm)

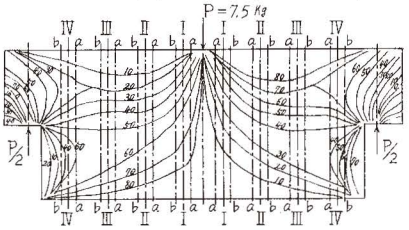

(a) Isoclinics in the Case of $P=7.5$ kg

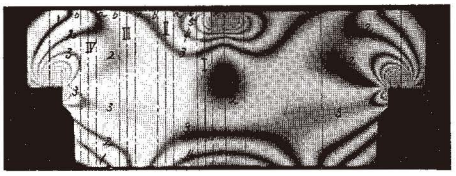

(b) Stress Patterns in the Case of $P=70.0$ kg

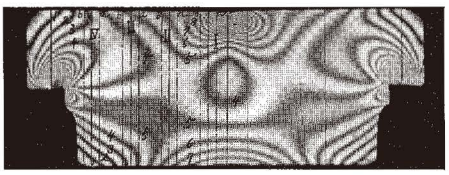

(c) Stress Patterns in the Case of $P=124.0$ kg

Fig. 14. Isoclinics and Stress Patterns of the Beam Model B_5 Bearing a Concentrated Line Load.

Model C_1 ($h=1.0$ cm, $l=9.0$ cm)

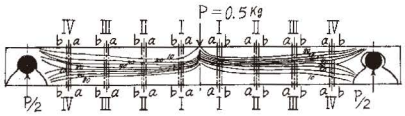

(a) Isoclinics in the Case of $P=0.5$ kg

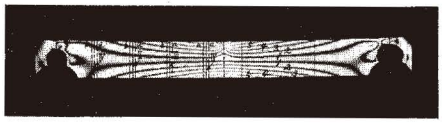

(b) Stress Patterns in the Case of $P=5.0$ kg

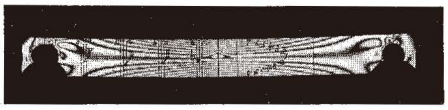

(c) Stress Patterns in the Case of $P=7.5$ kg

Fig. 15. Isoclinics and Stress Patterns of the Beam Model C_1 Bearing a Concentrated Line Load.

Model C_2 ($h=1.5$ cm, $l=9.0$ cm)

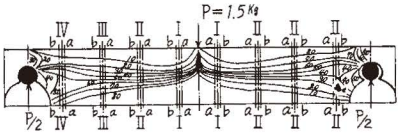

(a) Isoclinics in the Case of $P=1.5$ kg

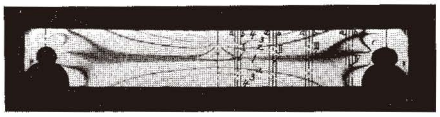

(b) Stress Patterns in the Case of $P=10.0$ kg

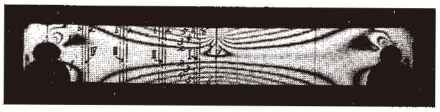

(c) Stress Patterns in the Case of $P=12.5$ kg

Fig. 16. Isoclinics and Stress Patterns of the Beam Model C_2 Bearing a Concentrated Line Load.

Model C_3 ($h=2.0$ cm, $l=9.0$ cm)

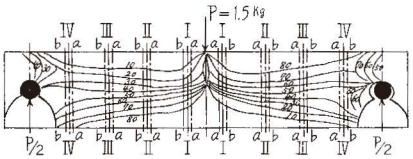

(a) Isoclinics in the Case of $P=1.5$ kg

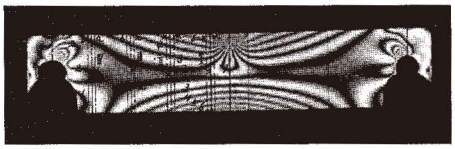

(b) Stress Patterns in the Case of $P=25.0$ kg

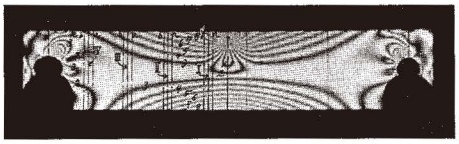

(c) Stress Patterns in the Case of $P=32.5$ kg

Fig. 17. Isoclinics and Stress Patterns of the Beam Model C_3 Bearing a Concentrated Line Load.

Model C_4 ($h=3.0$ cm, $l=9.0$ cm)

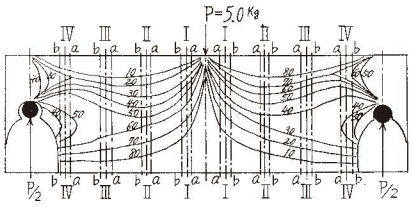

(a) Isoclinics in the Case of $P=5.0$ kg

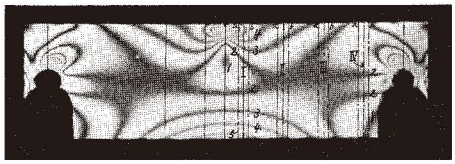

(b) Stress Patterns in the Case of $P=40.0$ kg

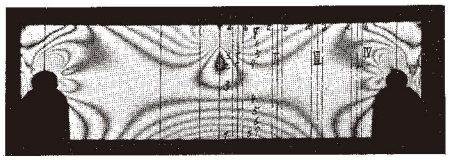

(c) Stress Patterns in the Case of $P=70.0$ kg

Fig. 18. Isoclinics and Stress Patterns of the Beam Model C_4 Bearing a Concentrated Line Load.

Model C_5 ($h=4.0$ cm, $l=9.0$ cm)

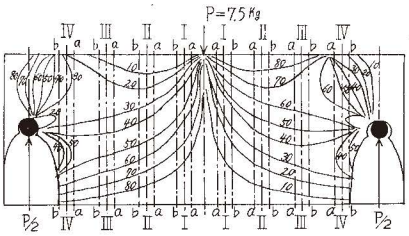

(a) Isoclinics in the Case of $P=7.5$ kg

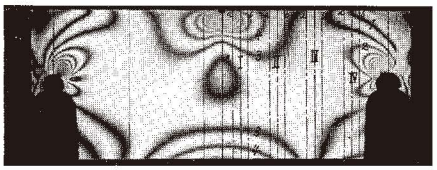

(b) Stress Patterns in the Case of $P=70.0$ kg

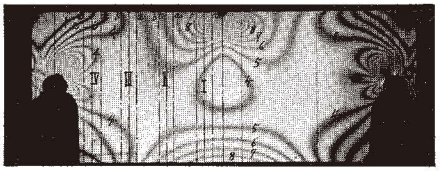

(c) Stress Patterns in the Case of $P=124.0$ kg

Fig. 19. Isoclinics and Stress Patterns of the Beam Model C_5 Bearing a Concentrated Line Load.

(1) Stress analytical formulae of the Shear Difference Method

He got the stress distributions of τ_{yx}, σ_x, σ_y on the base of the above-mentioned isoclinics and stress patterns by using the next formulae based on the principle of stress analysis.

$$\tau_{yx}=\frac{1}{2}(\sigma_1-\sigma_2)\sin 2\theta$$

$$\sigma_y=(\sigma_y)_0-\Sigma\Delta\tau_{yx}$$

$$\sigma_x=\sigma_y-(\sigma_1-\sigma_2)\cos 2\theta$$

(1)

However, $\sigma_1-\sigma_2$: Principal stress difference $=(S/d)_n$ (kg/mm^2)
S: Fringe stress (kg/mm)
n: Degree of stress patterns
d: Thickness of model (mm)
$(\sigma_y)_0$: σ_y of upper fringe when $y=0$ (kg/mm^2)
θ: Angle between load line and principal stress axis (degree)
$\Delta\tau_{yx}$: Difference of τ_{yx} in the cross section at interval of Δ_x (kg/mm^2)

(2) Theoretical calculating formulae

The theoretical formulae published by Mr. M. M. Frocht on the rectangular simple beam with equall cross sections are shown as follows:

$$\sigma_y=-\frac{2P}{d}\cdot\frac{1}{\pi}\cdot\frac{y^3}{(x^2+y^2)^2}$$

$$\sigma_x=\frac{2P}{d}\left\{\frac{3}{h^3}\left(\frac{l}{2}-x\right)\left(y-\frac{h}{2}\right)-\frac{1}{\pi}\cdot\frac{x^2y}{(x^2+y^2)^2}\right\}$$

$$\tau_{yx}=-\frac{2P}{d}\left\{\frac{3}{2h^3}(hy-y^2)+\frac{1}{\pi}\cdot\frac{xy^2}{(x^2+y^2)^2}\right\}$$

(2)

However, l: Span length (mm)
h: Height of beam (mm)
d: Thickness of model (mm)
x: Horizontal distance of any point measured from the centre of span (mm)
y: Vertical distance of any point measured from the upper surface

The above-mentioned formulae have been made by combining the initial beam theory and the radial stress theory, assuming that the rectangular beam is one part of semiinfinite plate.

These calculating results are obtained by the summation of the common stress of simple beam and the radial additional secondary stress radiated from the top of the centre of span.

From the calculating results, the writer has clarified that the difference between results calculated by the common beam theory and the above-mentioned theory is very little.

III. On the Results of Experimental Analysis

1. Photoelastic stress distributions

The shearing stress distributions τ_{yx} and the axial stress distributions σ_x at the cross sections I–I, II–II, III–III and IV–IV of each model are shown in Fig. 20～Fig. 25.

(1) Distributions of shearing stress intensities τ_{yx}

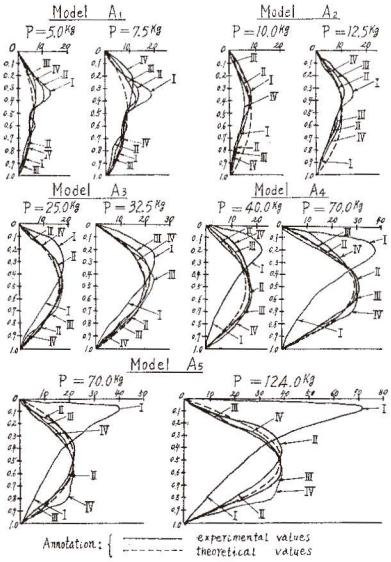

Fig. 20. Shearing Stress Intensities τ_{yx} of A-Type Models. (kg/cm²)

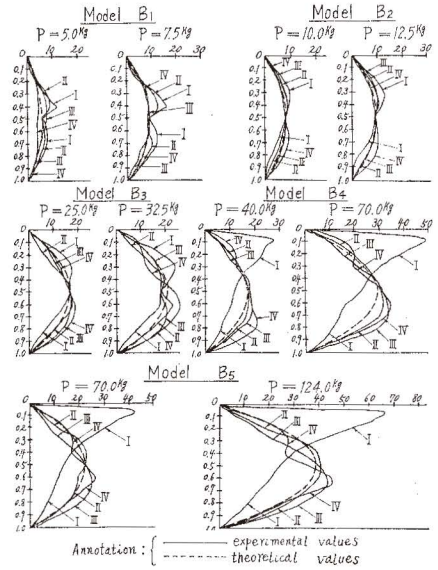

Fig. 21. Shearing Stress Intensities τ_{yx} of B-Type Models. (kg/cm²)

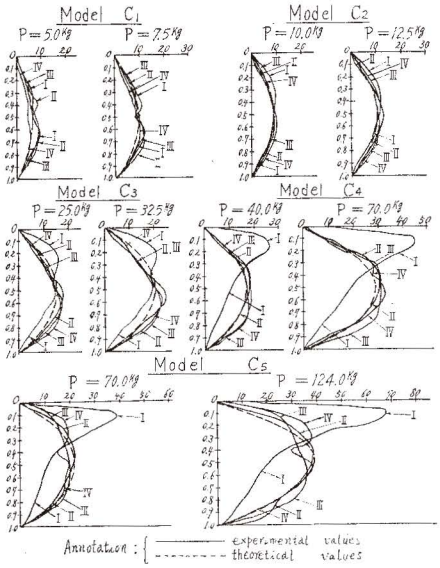

Fig. 22. Shearing Stress Intensities τ_{yx} of C-Type Models. (kg/cm²)

(2) Distributions of axial stress intensities σ_x

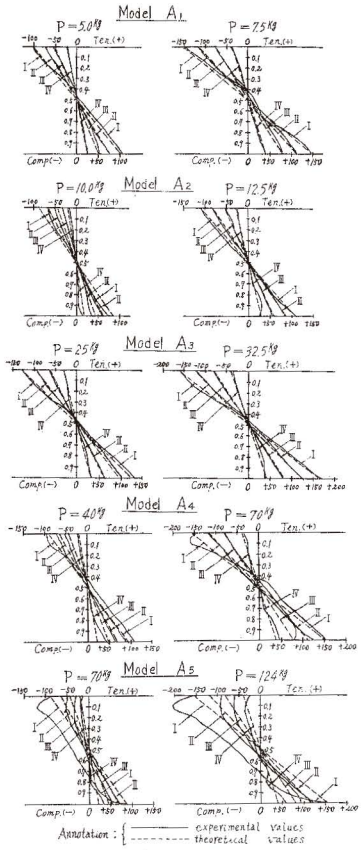

Fig. 23. Axial Stress Intensities σ_x of A-Type Models. (kg/cm²)

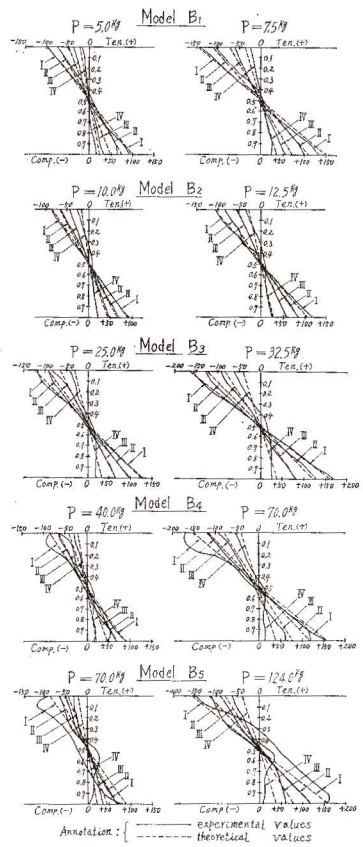

Fig. 24. Axial Stress Intensities σ_x of B-Type Models. (kg/cm²)

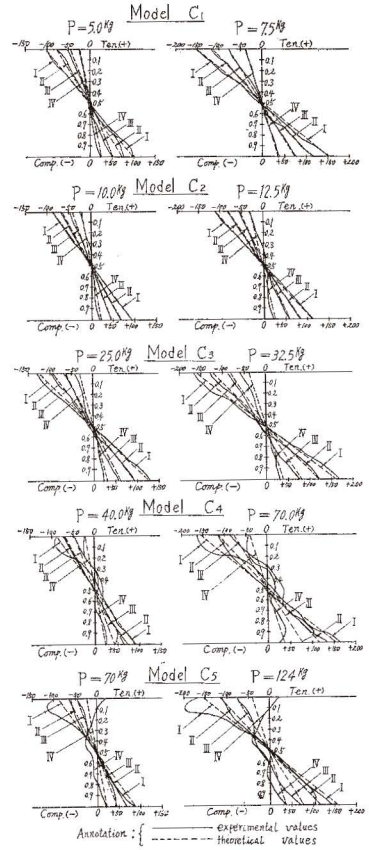

Fig. 25. Axial Stress Intensities σ_x of C-Type Models. (kg/cm²)

(3) $\sigma_{max}/\sigma_{nom}-l/h$ Curves

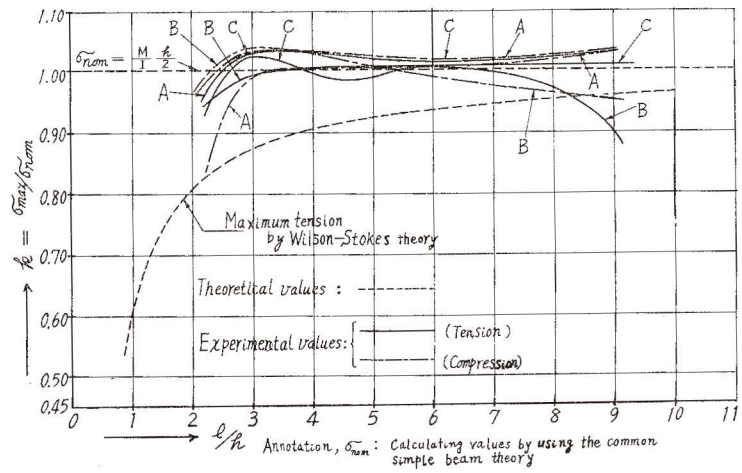

Fig. 26. $\sigma_{max}/\sigma_{nom}-l/h$ Curves.

2. Deflections at the centre of span and fibre strains on the upper and lower surfaces

(1) Deflections

The present writer has exactly measured the vertical displacements on the intersections of the vertical centre and support lines of span and the horizontal central axis line by using two reading microscopes, and from the differences of their vertical displacements he has decided the minute deflections at the centre of span.

Then, he has obtained the Load-Deflection Curves shown in Fig. 27.

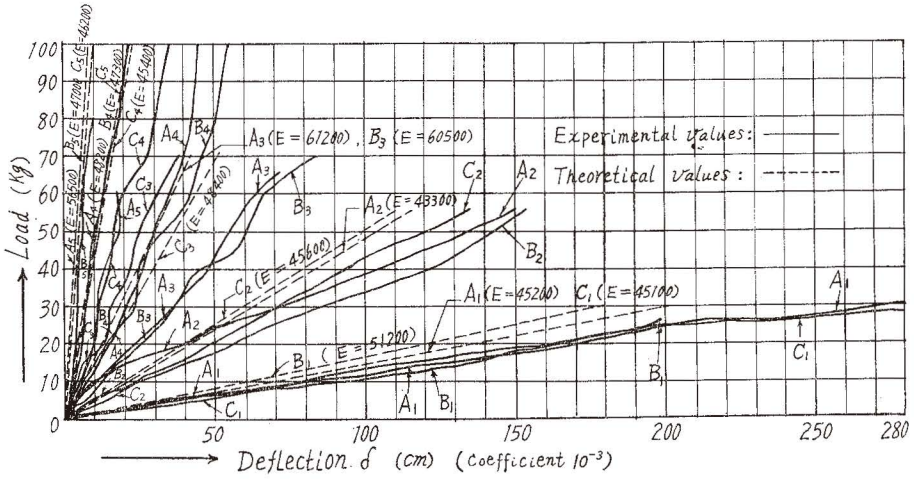

Fig. 27. Load-Deflection Curves. (Deflections at the Centre of Span)

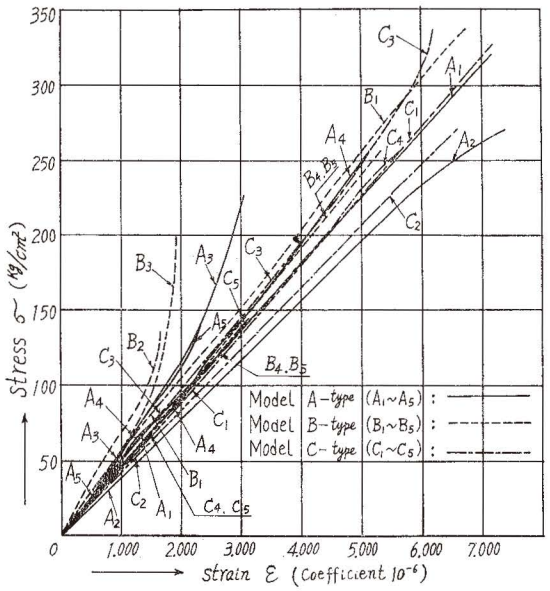

Fig. 28. Stress-Strain Curves. (Measured at the Centre of Span)

(2) Edge fibre strains

He has measured the strains of gages at the middle part shown in Fig. 1 by using a strain meter and showed the relations of those experimental strain values in Fig. 28.

3. Modulusli of flexural elasticity

He has obtained each of the modulusli of flexural elasticity, flexural tensile elasticity, and flexural compressive elasticity by using the Load-Deflection Curve and Stress-Strain Curve, and expressed the relation of E_b and l/h by E_b-l/h Curve shown in Fig. 29.

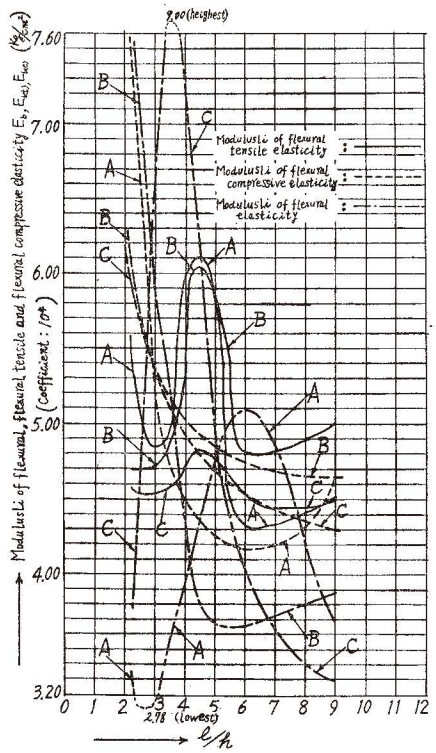

Fig. 29. E_b-l/h Curves. (Measured at the Centre of Span)

4. Horizontal displacement of supporting points and horizontal strains by the expansion and contraction of the central axis.

He has exactly measured the horizontal displacement of the supporting and central points of span on the central axis line by using 2 Reading Microscopes and strictly decided the horizontal displacement Δl at the supporting points by using the difference of the above-mentioned horizontal displacements.

Still more, he has calculated the expansion and contraction values of the central axis line between both supports by using the values of vertical displacements δ_v, assuming that the deflection curves of beams would become parabolas.

Table 1. Values of the Expansion and Contraction of the Span on the Central Axis.

Models	Loads P (kg)	Horizontal displacements of supporting points Δl (cm)	Vertical displacements of central point δ_v (cm)	Lengths of span on central axis l' (cm)	Expansion and contraction values of span on central axis $l'-l$ (cm)
A_1	5.0	+0.015	+0.035	9.030	+0.030
	30.0	+0.003	+0.280	9.024	+0.024
A_2	10.0	−0.006	+0.009	8.988	−0.012
	55.0	−0.045	+0.149	8.914	−0.086
A_3	25.7	−0.026	+0.032	8.948	−0.052
	70.0	−0.081	+0.098	8.840	−0.160
A_4	40.0	+0.024	+0.178	9.056	+0.056
	70.0	−0.001	+0.181	9.006	+0.006
	100.0	−0.022	+0.232	8.968	−0.032
A_5	70.0	−0.026	+0.015	8.948	−0.520
	100.0	−0.023	+0.004	8.954	−0.046
B_1	5.0	−0.012	+0.038	8.976	−0.024
	30.0	−0.029	+0.194	8.950	−0.050
B_2	10.0	−0.015	+0.032	8.970	−0.030
	55.0	−0.023	+0.153	9.048	+0.048
B_3	25.0	+0.006	+0.032	9.012	+0.012
	70.0	−0.026	+0.085	8.950	−0.050
B_4	40.7	−0.038	+0.012	8.924	−0.076
	70.0	−0.052	+0.015	8.896	−0.104
	100.0	−0.077	+0.039	8.846	−0.154
B_5	70.0	−0.054	+0.007	8.892	−0.108
	100.0	−0.078	+0.003	8.844	−0.156
C_1	5.0	−0.026	+0.045	8.948	−0.042
	27.5	−0.045	+0.278	8.928	−0.072
C_2	10.0	−0.014	+0.025	8.972	−0.028
	55.0	−0.042	+0,061	8.916	−0.084
C_3	25.0	−0.016	+0.013	8.968	−0.032
	70.0	−0.060	+0.039	8.888	−0.120
C_4	40.0	−0.037	+0.003	8.926	−0.074
	70.0	−0.057	+0.010	8.886	−0.114
	100.0	−0.106	+0.023	8.788	−0.212
C_5	70.0	−0.049	+0.015	8.902	−0.098
	100.0	−0.083	+0.022	8.834	−0.164

Annotation, Mark of δ_v (+): Vertical displacement of load direction
Mark of Δl (+): Horizontal expansion, Mark of Δl (−): Horizontal contraction

Table 2. Average Values of the Expansion and Contraction of the Span on the Central Axis of Each Model.

Models	Extent of loads P (kg)	Average lengths of span on central axis l' (cm)	Average values of expansion and contraction of span on central axis $l'-l$ (cm)
A kind	5.0~100.0	8.971	−0.029
B "	5.0~100.0	8.937	−0.063
C "	5.0~100.0	8.948	−0.052

See Table 1 and Table 2.

5. Breaking loads and the maximum stress intensities of some cross sections

The results of breaking test on each model are shown as follows.
See Table 3.

Table 3. Breaking Loads and Maximum Stress Intesities in the Central Cross Section.

Model	Breaking loads P_K (kg)	Maximum berding stress intensities in breaking loads σ_{max} (kg/cm²)	Maximum shearing stress intensities in breaking loads τ_{max} (kg/cm²)	Breaking phenomenons
A_1	45.0	±1,012.5	112.5	Central bending moment
A_2	140.0	±1,400.0	234.0	"
A_3	320.0	±1,800.0	401.0	"
A_4	650.0	±1,624.0	542.0	"
A_5	780.0	±1,096.0	488.0	"
B_1	45.0	±1,012.5	225.0	Central bending moment
B_2	160.0	±1,600.0	534.0	Central bending moment End shearing force
B_3	160.0	± 900.0	401.0	End shearing force
B_4	200.0	± 500.0	333.0	"
B_5	240.0	± 337.4	300.0	"
C_1	60.0	±1,350.0	251.0	Central bending moment
C_2	180.0	±1,800.0	410.0	Central bending moment End shearing force
C_3	120.0	± 675.0	187.5	Central bending moment
C_4	520.0	±1,300.0	500.0	End shearing force
C_5	720.0	±1,013.0	500.0	"

IV. Consideration

1. Distributions of the photoelastic stress intensities

(1) Distributions of the shearing stress intensities τ_{yx}

In the shearing stress distributions at the cross sections near supporting points of any model of A, B, and C kinds, the maximum experimental stress intensities

are larger than those of the theoretical calculation and those phenomena become so more remarkable as the load and height of beams increase.

Then, the present writer has found that these stress phenomena agree totally with the results investigated by some research workers, and he has also found that in the case of Type-1 and Type-2 models with small height for span the maximum shearing stress intensities of C_1 and C_2 models are smaller than those of A_1, A_2, B_1 and B_2 models and these distributions of stress intensities are close to the theoretical calculating curves.

It seems that these phenomena are caused by the different construcfions of supports.

(2) Distributions of the axial stress intensities σ_x

The present writer has clarified that the experimental axial stress distributions at the cross sections near a loading point become fairly larger than those of the theoretical calculation, and that these phenomena are more remarkable as the load and height of beams increase.

These tendencies have also concured totally with the results investigated by some research workers and he has proved also that the stress distribution curves of A and B kind models with large beam heights for span show the pretty unbalanced changeable disturbances as compared with those of C kind models with the different constructions of supports.

Then, it is worth notice that in A and B kind models the differences of experimental and theoretical interior stress distributions are very remarkable as compared with those of fibre stress intensity, and the greater the model height is the more this phenomenon is remarkable.

(3) $\sigma_{max}/\sigma_{nom}-l/h$ Curves

In this study the present writer has mainly treated models with the extent of beam heights $h/l=0.111\sim0.444-l/h=2.25\sim9.0$ used usually in the bridge and the other similar construction, and found that in the extent of $l/h=3\sim7$, $\sigma_{max}/\sigma_{nom}-l/h$ Curves obtained by this experiment are very close to the results calculated by the Common Simple Beam Theory as the figures show.

Specially in B kind models with the extent of $l/h=7\sim9$ the experimental tensile and compressive stress intensities σ_t, σ_c are about $5\sim10\%$ smaller as compared with the theoretical values, and in A kind models with the extent $l/h=2.25\sim2.5$ the experimental compressive stress intensities σ_c are about $10\sim17\%$ smaller as compared with the theoretical values.

It seems that these differences are caused by the different constructions of supports.

But it is worth notice that the stress phenomena of $\sigma_{max}/\sigma_{nom}-l/h$ Curves of any model beam are pretty different from the results calculated by using the Theory of Wilson-Stokes.

These stress phenomena were proved also from the other experimental results investigated specially by the present writer on 15 model beams of A kind.

On the contrary, it seems that in the models with the beam height of the above-mentioned extent $l/h=2.25\sim9.0$ the experimental fibre stress intensities will be not very different from the values calculated by using the Common Simple Beam Theory.

Then it is proved also from the values calculated by the Scheibe Theory in books of Mr. K. Girkmann and Mr. K. Beyer that the experimental fibre stress intensities of models with the beam height in the extent of $h/l<0.5$ $(l/h>2.0)$ are not very different from the values calculated by using the Common Simple Beam Theory.

The Theory of Wilson-Stokes was made up by using the hyperbola, assuming that $k=\sigma_{max}/\sigma_{nom}=1.0$ was largest and the more the value of l/h grew larger (the beam grew smaller in height), the more the value of $k=\sigma_{max}/\sigma_{nom}$ came nearer to 1.0.

It seems that this theory built up by using the hyperbola is too ideal, but the present writer cannot deny that $\sigma_{max}/\sigma_{nom}-l/h$ Curves of models with the larger beam height in the extent of $h/l>0.5$ show approximately the avove-mentioned hyperbola and he pays his respects to the observation of Mr. Wilson-Stakes regarding the theory on the very deep beam.

But according to the latest study he clarified noticeably that in some extents of l/h the fibre stress intensities of deep beam models were merely larger than the values calculated by the Common Simple Beam Theory.

The curves of $\sigma_{max}/\sigma_{nom}-l/h$ in A and B kinds models have especially shown the disturbed and variable phenomena compared with those of C kind models.

He concluded that these above-mentioned phenomenons were caused by the difference of supported constructions.

2. Deflections at the centre of span and fibre strains on the upper and lower surfaces

(1) Deflections

The present writer measured at the same time the deflections in the central point and supported points, and he calculated the exact deflections by using the difference of the central and support's deflections and found that the vertical compressive strain of the supported points had grown considerably large.

Then, he clarified collectively that the experimental deflections of all models were larger than the theoretical calculating values of them, and could prove the above-mentioned tendency also by his other investigated results.

He showed as noticeable phenomena that the experimental deflections of C kind of models came most near the theoretical calculating ones and found that the above-mentioned phenomena were caused by the fact that the supporting constructions of C kind of models had come most near those of the theoretical ideal simple beam.

From the close examination, he found the fact that every deflection of A, B, and C kind of models did not show a great difference in the extent of models with very small beam height but in the deep beam models the stress intensities

and deflections of A, B and C kind of models showed a special character caused by the difference of supporting constructions in each kind of models.

He found also that in the most deep beam models of $l/h=2.25$, each magnitude of central deflections was shown in order of A, B and C kind of models, but it seems that the order of each magnitude of central deflections will be changeable in the new models with the deeper height, because the stress phenomena of the Scheibe Theory are caused in these new deeper beam models.

(2) Edge fibre strains

From Stress-Strain Curves he found the fact that the rate of strain ε for stress σ of B kind of models was smaller compared with those of A and C and concluded that these phenomena were caused by the influence of special constructions of supports with the notches.

3. Modulusli of flexural elasticity

In this study the present writer could examine closely how the modulus of flexural elasticity was influenced by the change of l/h and he couly prove that the modulus of flexural elasticity, flexural tensile elasticity and flexural compressive elasticity severally showed the peculiar changeable tendency.

From the synthetic view point, he found that the modulusli of flexural elasticity were most changeable and these values reached from the largest, 90,000 kg/cm^2 to the smallest, 27,800 kg/cm^2.

Then, in coparison with A, B and C kind of models he found approximately that Elaticity—l/h Curves in every kind elasticity showed the abrupt changeable shape with the extent of $h/l=0.167\sim0.286$ $(l/h=6.0\sim3.5)$.

He clarified also by the close examination that in each kind of beam models the curves of the modulusli of flexural tensile elasticity and flexural compressive elasticity showed the shape of same tendency but the curves of modulusli of flexural elasticity showed a different changeable shape only in B kind models.

He concluded that these phenomena were caused by the influence of special constructions of supports with notches.

Still more, these changeable phenomena on modulusli of flexural elasticity are proved also by the results with the same tendency in his other experiments.

4. Horizontal displacement of supporting points and axial strains by the expansion and contraction of the central axis line between both supports.

He clarified that in each of A, B and C kind of models the axial strain of the central axis line between both supports came out as the contraction all but two or three exceptions.

That is to say, the average value of each kind and the total average value of models is as follows.

Average value of A kind of models: -0.029 cm (Contraction)
Average value of B kind of models: -0.063 cm (Contraction)
Average value of C kind of models: -0.052 cm (Contraction)
Total average value: -0.048 cm (Contraction)

These facts are proved presumedly also by the other close examination on the expansion or contraction of beam models in which the axial resultant force of each cross section was obtained severally by the graphical calculation of stress intensities and the total strain of each beam model was calculated on the whole as the contraction all but two or three models.

He found that the pretty large contraction of B kind models was caused by the special contstructions of both supports.

It seems that the tensile fibre strain of the lower surface in the span centre of B kind of models was decreased by the influence of both supports with the notches, because the above-mentioned tensile fibre strain of B kind models was considerably smaller compared with those of A and C kind models in the Stress-Strain Curves.

5. Breaking loads and the maximum stress intensities of some cross sections

In the 1-Type and 2-Type models with the beam small in height the large difference was nonexistent between each breaking load of A, B and C kind models but from the close examination he found that the breaking load of C kind models was largest compared with those of A and C kind models.

These beraking phenomena can be explained by the fact that the shearing stress intensities of 1-Type and 2-Type models is secondary and by far smaller compared with the axial stress intensities of the same models because the cross sections of those beam models (1-Type and 2-Type) are comparatively small.

In the 3-Type, 4-Type and 5-Type models with the beam large in height the breaking load of A kind models was largest compared with those of B and C kind models because A kind models will be broken by the central bending moment, and the next amount of breaking load was in order of C and B kind models.

He felt interested in the fact that the breaking load of B_4 and B_5 models large in height was very smaller compared with those of A and C kind models.

It is estimated clearly that these phenomena were caused by the influence of end shearing force at supports.

If the beam model is made by the material that its bending, tensile, compressive and shearing strength are as nearly equal to each other as steel, its maximum bending stress intensity will generally give a breaking strength of the material.

But it seems that the above-mentioned phenomena of beam models constructed of epoxy resin are reasonable beacause the bending, tensile, compressive and shearing strength of epoxy resin are very different to each other.

Still more, it is desirable that the notch's shape at the supporting parts of beam with variable cross sections is made by using the easy slope avoiding the steep slope, because the beam models with variable cross sections of easy slope have unexpected strength.

These facts are proved by the present writer's investigations on the beam with variable cross sections and the experiments on the timber beams of Mr. King and Langlans.

The C_3 beam model was broken by the central bending moment of the concentrated line load $P=120$ kg at the centre of span and from the above-mentioned view-point, he found that the breaking strength of epoxy resin was variable according to the quality of material and even the slight flaw gave a very bad influence to the breaking strength of beam models.

He could conclude that the beam models having notches at the supporting parts were broken according to the Maximum Shear Theory—$\tau_{max}=\sqrt{(\sigma_x/4)^2+\tau_s^2}$, because it was clarified by his experiments that the break by shear of models with notches at the supporting parts grew oblique by the diagonal tension.

It was found that the bending breaking strength of photoelastic epoxy resin used in his experiment and designated by Riken Meter Company was considerably large as shown in Table 3.

He presumed that its shearing breaking strength is about 0.30～0.40 of the above-mentioned bending breaking strength.

Furthermore, there are few materials for studies on the breaking strength of photoelastic epoxy resin but many materials for those of epoxy resin of binding agent.

Then, he found that the breaking strength of binding agent's epoxy resin was by far smaller than those of photoelastic epoxy resin.

V. Conclusion

The present writer measured as strictly as possible the photoelastic stress distributions, the vertical and horizontal displacements of the central point and supporting points, the bending tensile and compressive fibre strains of the central point and the breaking load endeavoring to minimize the measuring errors, so he has obtained the good results beyond expectation where there are hardly any measuring errors and could achieve his first purpose of study.

Still more, it is to be desired that the better measuring method is advanced and developed in future.

In the model beams of three kinds A, B and C, the stress distributions, displacements and modulusli of flexural elasticity of C kind models were most close to the theoretical calculated values of simple beam because the C kind beam models were most similar to the ideal type of theoretical simple beam.

But he could prove positively that the more the height of beam models grew deep for the span the more the above-mentioned experimental values of each kind beam models with the deep height became different compared with the theoretical calculated values, and that especially the measuring and experimentally analytical results of A kind model beams with the deep height were very different from the theoretical calculated values of simple beam.

It seems that these differences are caused by the fact that the supporting points are at the bottom surface of beam models.

This conclusion can be clearly proven also by the results of his other experi-

ments. Then it is worthy of notice that by the influence of supports with the notches the stress phenomena of B kind beam models are different from those of A and C kind beam models without the notches.

He clarified also the fact that the tendency of these phenomena on the stress distributions and displacements concurred with it of the results of his experiments on steel beam models.

Still more, he clarified the minute and interesting fact that the influence of the difference supporting construction acted delicately on the variable curves of the stress distributions, displacements and modulusli of flexural elasticity.

Acknowledgement

The present writer is obliged to express his sincere thanks to some graduates of Civil Engineering Department of Muroran Institute of Technology, for their kind cooperation in this study.

(Received Apr. 18, 1967)

References

1) S. Timoshenko: Theory of Elasticity, 27, 52 (New York, 1934).
2) Tatsuzo Fukuhara: Memoirs of the Society of Mechanical Engineering, **30**-123,365 (Tokyo, 1927).
3) M. M. Frocht: Photoelasticity, Vol. I, 252 (New York, 1949), Vol. II, 104 (New York, 1948).
4) E. G. Coker, L. N. G. Filon: A Treatise on Photoelasticity, 458 (London, 1957).
5) Sakutaro Nakamura, Isao Bansho: The Colloction of Summaries, in the 17th Science Lecture Meeting of Japan Society of Civil Engineering, **I**-78, 165 (Tokyo, 1962), The Collection of Summaries in the 12th Japan National Congress for Applied Mechanics, **I**-124 43 (Tokyo, 1964).
6) K. Girkmann: Flächentragwerke, 18 (Wien, 1963).
7) K. Beyer: Die Statik in Stahlbetonbau, 712 (Berlin, 1956).
8) E. Mönch: Proceedings of the Society for Experimental Stress Analysis **21**-1, 141 (Westport, 1964).
9) J. P. Lee: Journal of Applied Mechanics **29**-E. 4, 696 (New York, 1962).
10) П. И. Аакксеев: СТРОИТЕАВНА МЕХАНИКА И РАСЧЕТ СООРУЖЕНИЙ № 6, 37 (МОСКВА, 1963).
11) Jiro Tsuji, Masataka Nishida, Kozo Kawada: Experimental Method of Photoelasticity, 1 (Tokyo, 1965).
12) Technical Society for the Study of Stress Measurement: The Method of Stress Measurement, 472 (Tokyo, 1955).
13) Sakutaro Nakamura, Isao Bansho: Memoirs in the Hokkaido Branch of the Japan Society of Civil Engineering, No. 19, 56 (Sapporo, 1963).
14) Sakutaro Nakamura, Isao Bansho: The Collection of Summaries in the 19th Science Lecture Meeting of Japan Society of Civil Engineering, **I**-48, 48 (Tokyo, 1964).
15) M. Nishida, H. Saito: Proceedings of the Society for Experimental Stress Analysis, **21**-2, 366 (Westport, 1964).
16) H. T. Jessop, F. C. Harris: Photoelasticity Principles & Method, 1 (London, 1949).